

# Predicting Intraoperative Hypoxemia with Joint Sequence Autoencoder Networks

Hanyang Liu, Michael Montana, Dingwen Li, Thomas Kannampallil, Chenyang Lu

Washington University in St. Louis

{hanyang.liu, montanam, dingwenli, thomas.k, lu}@wustl.edu

## Abstract

We present an end-to-end model using streaming physiological time series to accurately predict near-term risk for hypoxemia, a rare, but life-threatening condition known to cause serious patient harm during surgery. Our proposed model makes inference on both hypoxemia outcomes and future input sequences, enabled by a joint sequence autoencoder that simultaneously optimizes a discriminative decoder for label prediction, and two auxiliary decoders trained for data reconstruction and forecast, which seamlessly learns future-indicative latent representation. All decoders share a memory-based encoder that helps capture the global dynamics of patient data. In a large surgical cohort of 73,536 surgeries at a major academic medical center, our model outperforms all baselines and gives a large performance gain over the state-of-the-art hypoxemia prediction system. With a high sensitivity cutoff at 80%, it presents 99.36% precision in predicting hypoxemia and 86.81% precision in predicting the much more severe and rare hypoxemic condition, persistent hypoxemia. With exceptionally low rate of false alarms, our proposed model is promising in improving clinical decision making and easing burden on the health system.

## 1 Introduction

Hypoxemia, or low blood oxygen saturation ( $\text{SpO}_2$ ), is an adverse physiological condition known to cause serious patient harm during surgery and general anaesthesia [Dunham *et al.*, 2014]. Without early intervention, prolonged hypoxemia can seriously affect surgical outcomes, associated with many adverse complications such as cardiac arrest, encephalopathy, delirium, and post-operative infections [Lundberg *et al.*, 2018]. To mitigate the effects of hypoxemia, anesthesiologists monitor  $\text{SpO}_2$  levels during general anesthesia using pulse oximetry, so that actions can be taken in a timely manner. Despite the availability of physiological sensors for real-time monitoring, reliable early prediction of hypoxemic events remains elusive [Ehrenfeld *et al.*, 2010].

In recent years, data from electronic health records (EHR) are used to develop predictive models to anticipate risks of

future diseases or potential instability, facilitating early interventions to mitigate the occurrence of adverse events [West *et al.*, 2016]. Similar attempts [ElMoaqet *et al.*, 2016; Erion *et al.*, 2017] have been made to target hypoxemia based on  $\text{SpO}_2$  data. Recently, [Lundberg *et al.*, 2018] proposed Prescience, a gradient boosting machine (GBM)-based method for predicting intraoperative hypoxemia by integrating a number of preoperative static variables and intraoperative physiological time series. Compared to prior works that only utilize  $\text{SpO}_2$ , the use of comprehensive patient data helps train a more reliable prediction model. However, as GBM cannot directly utilize multivariate time series, Prescience requires the extraction of hand-crafted features with limited capacity for capturing the temporal dynamics of a time series. In addition, the uniquely selected combination of features may not generalize to a new cohort from another hospital.

Another major limitation of the aforementioned hypoxemia models is that they were developed to target any low  $\text{SpO}_2$  occurrences where most of them are short-term (e.g., a single minute) and transient  $\text{SpO}_2$  reduction. In practice, most occurrences of low  $\text{SpO}_2$  do not necessarily reflect high patient risks for deterioration that actually require anesthesiologist intervention [Laffin *et al.*, 2020]. In contrast to transient  $\text{SpO}_2$  reduction, significant risks arise from *persistent hypoxemia*, defined as continuously low  $\text{SpO}_2$  over a longer time window (e.g., 10 minutes). Persistent hypoxemia can develop rapidly and unexpectedly due to acute respiratory failure, or other circumstances. It is immediately life-threatening if not treated [Mehta and Mehta, 2016]. For this study we have collected a large surgical dataset from a major academic medical center. In this cohort, despite the rareness (1.5% of all time) of low  $\text{SpO}_2$ , 24.0% of the surgical encounters experienced at least a single-minute  $\text{SpO}_2$  reduction (minutely sampled), while merely 0.9% experienced persistent hypoxemia. Unessential alarms can result in clinicians' desensitization to alarms, and thus the actually critical ones could possibly be missed. Hence, it is of high clinical importance to reliably predict *persistent hypoxemia*, which facilitates the most pivotal early interventions. However, the prediction of persistent hypoxemia is a greater challenge, as it is difficult for a machine learning model to learn reliable patterns from data with a certain class being underrepresented (0.04% labeled positive among all per-minute examples extracted from our dataset). Moreover, it requires the model to foresee longer-

term into the future, but the past data are decreasingly indicative of distal future outcomes.

We aim to address these challenges by developing an end-to-end learning framework that utilizes streaming physiological time series (e.g., heart rate, SpO<sub>2</sub>) and produces risk prediction of hypoxemia, while simultaneously learning powerful latent representation known to improve model robustness against class imbalance [Hendrycks *et al.*, 2019]. In addition to general hypoxemia (i.e., any SpO<sub>2</sub> reduction), we focus on predicting persistent hypoxemia given its clinical significance. Hypothetically, if we can foresee the future input data, especially the SpO<sub>2</sub> variation, we can anticipate the potential (persistent) hypoxemia more accurately. We propose a novel deep model, the hybrid inference network (hiNet) that simultaneously makes inference on both hypoxemia outcomes and future input sequences. This end-to-end model is enabled by jointly optimizing a modified LSTM autoencoder (LSTM-AE) that simultaneously reconstructs input and forecasts future input, and a discriminative decoder (classifier) trained for label prediction. With joint training, not only can the classifier leverage the learned latent representation, but also the supervisory signal from the classifier gets propagated to seamlessly direct representation learning towards optimizing the desired prediction task.

The proposed model is trained and evaluated on real-world patient data from pediatric surgeries from a large academic medical center. The data includes surgical information from 73,536 pediatric surgical encounters including around 118,000 hours of surgery time. The experiments show that our proposed model can reliably predict both general and persistent hypoxemia with a precision of 99.36% and 86.81% given a 80% sensitivity cut, which significantly outperforms all baselines including LSTM-AE based models, and gives a large performance gain (68.6% and 84.6% improvement in PR-AUC for general and persistent hypoxemia, respectively) over the state-of-the-art model for hypoxemia prediction. Specifically, our contributions are threefold:

- We propose a novel end-to-end sequence learning model that jointly optimizes a classifier for label prediction and an extended LSTM-AE for input reconstruction and forecast. Through joint training, the learned future-indicative latent representation facilitates better prediction and meanwhile seamlessly gets fine-tuned for task-specific effectiveness.
- To the best of our knowledge, our approach is the first to use a learning-based method for *persistent* hypoxemia prediction, a challenging but clinically significant problem.
- Extensive experiments on a large cohort show the effectiveness and significant improvement of our proposed model over strong baselines, with potential to improve clinical decision making and make impacts on surgical practice.

## 2 Related Works

### Learning to Predict Hypoxemia

Recently, several attempts have been made targeting hypoxemia using data-driven approaches. For instance, [ElMoaqet *et al.*, 2016] used a linear auto-regressive (AR) model on SpO<sub>2</sub> forecast. [Erion *et al.*, 2017] sought to use deep learning models such as LSTM to directly classify past SpO<sub>2</sub> data.

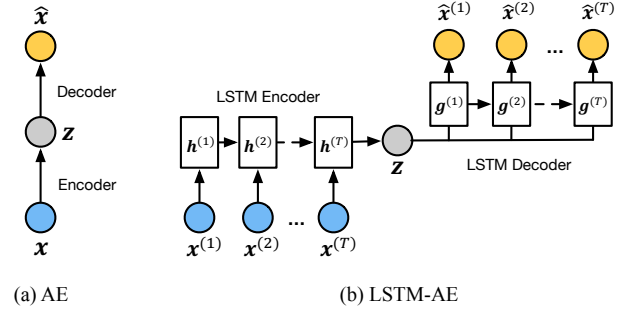


Figure 1: Generalized AE and LSTM-AE. In LSTM-AE, LSTM is used for both aggregation and disaggregation of sequential data.

[Nguyen *et al.*, 2018] used AdaBoost to identify false SpO<sub>2</sub> alarms, without directly targeting prediction. Recently, a more comprehensive approach, Prescience [Lundberg *et al.*, 2018], employed GBM to predict general hypoxemia based on both preoperative static variables and intraoperative time series. All these approaches aimed at either forecasting SpO<sub>2</sub> (regression) or predicting only general hypoxemia.

### Autoencoder-based Sequence Learning

Autoencoder (AE) [Davis and Goadrich, 2006], as shown in Figure 1(a), is widely used for representation learning. AE is trained to simultaneously optimize an *encoder* that maps input into latent representation, and a *decoder* that recovers the input by minimizing the reconstruction error. However, AE cannot directly handle sequential data. Recently, [Dai and Le, 2015] proposed a *seq2seq* AE by instantiating the encoder and decoder with LSTM, referred to as LSTM-AE, shown in Figure 1(b). [Srivastava *et al.*, 2015] further extended it to the composite LSTM autoencoder (LSTM-CAE) that additionally trains another decoder fitting future data as regularization. The LSTM-AE based methods have shown promising performance in learning representation for sequential data. For instance, [Laptev *et al.*, 2017; Zhu and Laptev, 2017] proposed to use pretrained LSTM-AE to extract deep features from time series for Uber trips and rare event forecasting. Recent clinical applications can be found in [Suresh *et al.*, 2017; Ballinger *et al.*, 2018; Baytas *et al.*, 2017] that used LSTM-AE to extract patient-level representation for phenotyping and cardiovascular risk prediction. These works are related to our approach, as they all use representation learning of pretrained LSTM-AE to facilitate a classification task. However, unsupervised pretraining tends to learn general task-agnostic underlying structure, and thus the greedy layer-wise optimization in separate steps can lead to a suboptimal classifier [Zhou *et al.*, 2014]. Instead, our approach relies on building an end-to-end model that jointly optimizes the classification and latent representation learning while balancing them more delicately.

## 3 Problem Formulation

Our dataset consists of  $N$  independent surgeries, denoted as  $\mathcal{D} = \{\mathcal{V}_i\}_{i=1}^N$ , where  $i$  is the index of surgeries, and  $\mathcal{V}_i$  is a set of time series inputs. We assume the time span is divided into equal-length time intervals. The multi-channel time series set

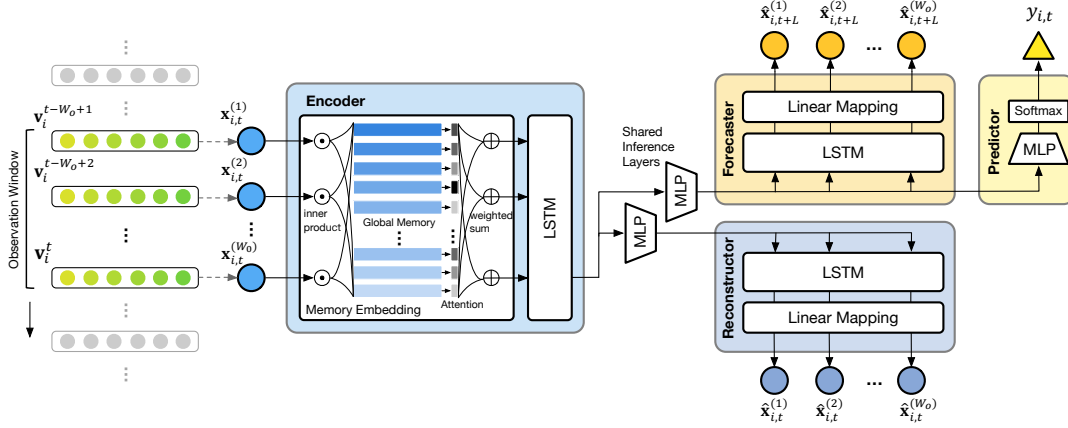


Figure 2: The end-to-end architecture of hiNet. The streaming data are fed into the memory-based encoder. The encoder-decoder network jointly optimizes the **Reconstructor** trained to recover input, the **Forecaster** trained to fit future input, and the **Predictor** to estimate labels.

$\mathcal{V}_i = [\mathbf{v}_i^1, \mathbf{v}_i^2, \dots, \mathbf{v}_i^{T_i}] \in \mathbb{R}^{V \times T_i}$ , where  $V$  is the number of time series channels,  $T_i$  is the length of surgery  $i$ , and  $\mathbf{v}_i^t \in \mathbb{R}^V$  is the vector of recorded data values at timestep  $t$ . For timestep  $t$ , we have a binary label  $y_{i,t} \in \{0, 1\}$ , where 1 indicates that a hypoxemic event will occur anytime within the next fixed-length time window  $[t+1, t+W_h]$ , otherwise  $y_{i,t} = 0$ .  $W_h$  denotes the prediction horizon. Given a new surgery  $i$  where the patient is not already in hypoxemia, and the data window  $\mathbf{X}_{i,t} = \mathcal{V}_i^{(t-W_o, t]} \in \mathbb{R}^{V \times W_o}$  at time  $t$  (zero padded if  $1 \leq t < W_o$ ), the goal is to train a classifier  $f$  that produces the label  $y_{i,t}$ :  $y_{i,t} = f(\mathbf{X}_{i,t})$ .

## 4 Proposed Model

Figure 2 shows an overview of our approach. This end-to-end framework jointly optimizes the desired classification task for prediction, and two auxiliary tasks for representation learning. The addition of the forecasting decoder contributes to learning future-related contextual representation. The joint training allows the supervised loss to direct representation learning towards being effective to the desired classification task. Hence, the joint integration of the three decoders enables the model to balance both extracting the underlying structure of data and providing accurate prediction.

### 4.1 Memory Augmented Sequence Autoencoder

When applying LSTM-AE on streaming time series using a sliding data window, the sequence encoder tends to learn mainly the local temporal patterns within the window. Recently, memory network [Sukhbaatar *et al.*, 2015; Gong *et al.*, 2019] has shown promising results in data representation. Generally, a memory network updates an external memory consisting of a set of basis features for look-up to preserve general patterns optimized on the whole dataset [Santoro *et al.*, 2016]. To help capture the global dynamics of physiological time series, we design a memory augmented LSTM-AE with two-step encoding of the input sequences.

#### Memory-based Encoding

Given a sliding window of time series  $\mathbf{X}_{i,t} = [\mathbf{x}_{i,t}^{(k)}]_{k=1}^{W_o} = [\mathbf{v}_i^{t-W_o+1}, \dots, \mathbf{v}_i^{t-1}, \mathbf{v}_i^t]$ , we first use a memory to embed the

input features of each step, and then use LSTM to aggregate all the embedded vectors within the window into one vector as representation, as shown in Figure 2.

*Stage 1: Global Memory Embedding.* We assume there are  $M$  feature basis vectors ( $M$  as a hyperparameter) for a specific dataset, and initialize a global memory  $\mathbf{B} = [\mathbf{b}_1, \mathbf{b}_2, \dots, \mathbf{b}_M] \in \mathbb{R}^{M \times V}$ . We assume that features of each step can all be embedded to a linear combination of the  $M$  feature bases. Given a feature vector  $\mathbf{x}^{(k)}$  of the  $k$ -th step, we obtain the attention  $\alpha$  for each basis  $\mathbf{b}_j$  by calculating the similarity of  $\mathbf{x}^{(k)}$  to each of them. The attention values are normalized by a softmax function:  $\text{Softmax}(z) = e^{z_k} / \sum_{k'} e^{z_{k'}}$ . Then the embedded vector is the sum of all the bases weighted by their attention. The memory  $\mathbf{B}$  is updated jointly with the network. Concretely,

$$\begin{aligned} \alpha_{i,t}^{(k)} &= \text{Softmax}(\mathbf{B}\mathbf{x}_{i,t}^{(k)}) \\ \mathbf{a}_{i,t}^{(k)} &= \sum_{j=1}^M \alpha_{i,t,j}^{(k)} \mathbf{b}_j \end{aligned} \quad (1)$$

*Stage 2: Local Sequence Aggregation.* Now we use an LSTM layer parameterized by  $\theta_h$  to capture the local temporal patterns within the embedded sequence. The last hidden state of the LSTM is used as the latent representation. With  $k \in [1, W_o]$ , the hidden state at each step and the final representation are:

$$\begin{aligned} \mathbf{h}_{i,t}^{(k)} &= \text{LSTM}(\mathbf{a}_{i,t}^{(k)}, \mathbf{h}_{i,t}^{(k-1)}; \theta_h) \\ \mathbf{z}_{i,t} &= \mathbf{h}_{i,t}^{(W_o)} \end{aligned} \quad (2)$$

For convenience, we denote this mapping from the input to the code space  $\Phi: \mathbb{R}^{V \times W_o} \rightarrow \mathbb{R}^Z$  as *Encoder* with trainable parameters  $\Theta_E = \{\mathbf{B}, \theta_h\}$ . We have  $\mathbf{z}_{i,t} = \Phi(\mathbf{X}_{i,t}; \Theta_E)$ .

#### Sequence Reconstructor

First the hidden representation  $\mathbf{z}$  is mapped to a new space using a multi-layer perceptron (MLP):  $\mathbf{q}_{i,t} = \text{MLP}(\mathbf{z}_{i,t}; \omega_q)$ . Then we copy the vector  $\mathbf{q}$  for every step  $k \in [1, W_o]$  as the input to the sequence disaggregation layers (i.e., an LSTM

and then a time-distributed linear layer as a surrogate of inverse memory) to reconstruct  $\hat{\mathbf{X}} = [\hat{\mathbf{x}}^{(1)}, \hat{\mathbf{x}}^{(2)}, \dots, \hat{\mathbf{x}}^{(W_o)}]$ :

$$\mathbf{g}_{i,t}^{(k)} = \text{LSTM}(\mathbf{q}_{i,t}, \mathbf{g}_{i,t}^{(k-1)}; \boldsymbol{\omega}_g) \quad (3)$$

$$\hat{\mathbf{x}}_{i,t}^{(k)} = \mathbf{g}_{i,t}^{(k)} \mathbf{W} + \mathbf{d} \quad (4)$$

We denote this mapping from the input space back to itself  $f_R : \mathbb{R}^{V \times W_o} \rightarrow \mathbb{R}^{V \times W_o}$  as *Reconstructor*. We have

$$\hat{\mathbf{X}}_{i,t} = f_R(\mathbf{X}_{i,t}; \boldsymbol{\Theta}_E, \boldsymbol{\Omega}_R) \quad (5)$$

where  $\boldsymbol{\Omega}_R = \{\boldsymbol{\omega}_q, \boldsymbol{\omega}_g, \mathbf{W}, \mathbf{d}\}$  represents the parameters of the sequence disaggregation layers. They can be learned by minimizing the loss:  $\mathcal{L}_R = \text{MSE}(\mathbf{X}_{i,t}, \hat{\mathbf{X}}_{i,t})$ .

## 4.2 Multi-decoder Joint Learning

Reconstructor in Eq. (5) helps learn latent representation that improves model robustness against class imbalance. However, Reconstructor may not provide enough future-indicative patterns that the prediction task relies on. Motivated to learn more future-related contextual representation, we propose the hybrid inference network (hiNet), which besides Reconstructor, jointly trains another auxiliary decoder for future input sequence forecast and a discriminative decoder for label prediction, as shown in Figure 2.

### Shared Inference Layers

Given the time series representation  $\mathbf{z}$ , first we map the representation  $\mathbf{z}$  to a new space through a new MLP parameterized by  $\boldsymbol{\Theta}_p$ :

$$\mathbf{p}_{i,t} = \text{MLP}(\mathbf{z}_{i,t}; \boldsymbol{\Theta}_p) \quad (6)$$

This vector  $\mathbf{p}$  will be shared as new encoded data representation used by both a sequence forecasting decoder and a classifier, so that the future-indicative representation learning and the classification can seamlessly benefit from each other.

### Sequence Forecaster

Given the new representation  $\mathbf{p}$ , now we build another sequence decoder to forecast the future (in  $L$  timesteps) input time series,  $\mathbf{X}_{i,t+L} = [\mathbf{x}_{i,t+L}^{(1)}, \mathbf{x}_{i,t+L}^{(2)}, \dots, \mathbf{x}_{i,t+L}^{(W_o)}] = [\mathbf{v}_i^{t+L-W_o+1}, \dots, \mathbf{v}_i^{t+L-1}, \mathbf{v}_i^{t+L}]$ . Similar to Eq. (3) and (4), we apply sequence disaggregation layers to the copied vectors  $\mathbf{p}$ . We denote the mapping from input to future input,  $f_F : \mathbb{R}^{V \times W_o} \rightarrow \mathbb{R}^{V \times W_o}$  as *Forecaster*. Hence

$$\hat{\mathbf{X}}_{i,t+L} = f_F(\mathbf{X}_{i,t}; \boldsymbol{\Theta}_E, \boldsymbol{\Theta}_p, \boldsymbol{\Omega}_F) \quad (7)$$

where  $\boldsymbol{\Omega}_F$  denotes the task-specific parameters in the sequence disaggregation layers. The parameters can be learned by minimizing the loss:  $\mathcal{L}_R = \text{MSE}(\mathbf{X}_{i,t+L}, \hat{\mathbf{X}}_{i,t+L})$ .

### Label Predictor

Given the new representation  $\mathbf{p}$  from Eq. (6) that contains indicative patterns of future data, now we build a classifier to predict the label  $y \in \mathbb{B}$ . We feed  $\mathbf{p}$  into an MLP with a softmax for the output. Using *Predictor* to denote the mapping  $f_P : \mathbb{R}^{V \times W_o} \rightarrow \mathbb{R}^{W_o}$ , and  $\boldsymbol{\Omega}_P$  to denote the task-specific MLP parameters, we have

$$\begin{aligned} \hat{y}_{i,t} &= \text{Softmax}(\text{MLP}(\mathbf{p}_{i,t}; \boldsymbol{\Omega}_P)) \\ &= f_P(\mathbf{X}_{i,t}; \boldsymbol{\Theta}_E, \boldsymbol{\Theta}_p, \boldsymbol{\Omega}_P) \end{aligned} \quad (8)$$

### Masked Predictor Loss

For a binary classifier, given true labels  $y \in \{0, 1\}$  and predicted probability  $\hat{y}$ , usually we use a cross-entropy loss

$$H(y, \hat{y}) = -y \log(\hat{y}) - (1 - y) \log(1 - \hat{y}) \quad (9)$$

For either the prediction of general or persistent hypoxemia, it's trivial and clinically less meaningful to predict the event when it already occurs, so we focus on predicting only the start of hypoxemia and leave the samples where hypoxemia already begins unlabeled (see Section 5.1 and Appendix A). To this end, a straightforward strategy is to directly exclude the unlabeled samples for both training and testing of the model, as in [Lundberg *et al.*, 2018; Erion *et al.*, 2017]. However, the unlabeled samples can still provide our model useful information indicative of SpO<sub>2</sub> tendency, and shape both Reconstructor  $f_R$  and Forecaster  $f_F$ . Instead, we propose a masked loss for Predictor. For surgery  $i$ , we have the binary mask vector  $\mathbf{m}_i = [m_{i,1}, m_{i,2}, \dots, m_{i,T_i}] \in \mathbb{B}^{T_i}$  where  $m_{i,t} = 0$  indicates surgery  $i$  at time  $t$  is in hypoxemia, otherwise 1. The modified Predictor loss is:

$$\mathcal{L}_P = \sum_i \sum_t H(m_{i,t} y_{i,t}, m_{i,t} \hat{y}_{i,t}) \quad (10)$$

In this way, the unlabeled data will be filtered out for Predictor but still used in training Reconstructor and Forecaster.

### Objective Function and Joint Training

Given  $\{(\mathbf{X}_{i,t}, y_{i,t}, m_{i,t})\}$  for  $i \in [1, N]$  and  $t \in [1, T_i]$ , we define the overall objective function to learn model parameters  $\{\boldsymbol{\Theta}_E, \boldsymbol{\Omega}_R, \boldsymbol{\Theta}_p, \boldsymbol{\Omega}_F, \boldsymbol{\Omega}_P\}$  for our end-to-end hybrid inference framework as minimizing the following joint loss:

$$\begin{aligned} \mathcal{L} &= \underbrace{\mathcal{L}_P}_{\text{label decoder}} + \beta \underbrace{(\mathcal{L}_F + \mathcal{L}_R)}_{\text{sequence decoders}} \\ &= \sum_i \sum_t \left[ H(m_{i,t} y_{i,t}, f_P(\mathbf{X}_{i,t}; \boldsymbol{\Theta}_E, \boldsymbol{\Theta}_p, \boldsymbol{\Omega}_P) \cdot m_{i,t}) \right. \\ &\quad \left. + \beta \|\mathbf{X}_{i,t+L} - f_F(\mathbf{X}_{i,t}; \boldsymbol{\Theta}_E, \boldsymbol{\Theta}_p, \boldsymbol{\Omega}_F)\|^2 \right] \\ &\quad + \beta \|\mathbf{X}_{i,t} - f_R(\mathbf{X}_{i,t}; \boldsymbol{\Theta}_E, \boldsymbol{\Omega}_R)\|_F^2 \end{aligned} \quad (11)$$

where  $\beta$  is the coefficient of Reconstructor and Forecaster,  $\boldsymbol{\Theta}_*$  denotes shared parameters, and  $\boldsymbol{\Omega}_*$  denotes task-specific parameters. The two sequence decoders  $f_R$  and  $f_F$  provide regularization to classifier  $f_P$  with optimized data representation and future-indicative patterns. Given the end-to-end architecture, we can jointly update all the parameters during training. After the joint model is trained, we only need Predictor  $f_P$  for label inference on new patients.

## 5 Experiment

We aim to present the experimental evaluation of hiNet by answering the following questions:

- **Q1:** Can hiNet improve the predictive performance for hypoxemic outcomes compared to baselines?
- **Q2:** How does each component such as memory embedding, and masked Predictor loss contribute to hiNet?
- **Q3:** How do the architecture and joint training benefit the representation learning in hiNet?

## 5.1 Data

Our real-world dataset originally consists of 79,142 surgical encounters from 2014 to 2018 with approximately 118,000 hours of surgeries in total (89 min per case in average), collected from a major academic medical center. Examples with recorded  $\text{SpO}_2$  of less than 60% were considered aberrant and excluded. We also excluded 5,606 cardiac surgery cases (with ICD-9 codes 745-747 and ICD-10 codes Q20-Q26), in which  $\text{SpO}_2$  levels were likely affected by the surgical procedure. After extensive data cleaning, there are 73,536 surgeries and  $V = 18$  channels of time series variables minutely sampled during surgical procedures. The prediction is run at every minute. We use carry-forward imputation for the missing values in a gap between two observations less than 20 min, and fill those that are never observed or haven't been observed for the past 20 min with zeros. All variables are normalized.

We evaluate the model on predicting both hypoxemic outcomes. **General hypoxemia** denotes any instance of  $\text{SpO}_2 \leq 90\%$  during surgery, and **persistent hypoxemia** is defined as  $\text{SpO}_2 \leq 90\%$  continuously for at least 10 min. We choose the  $\text{SpO}_2$  threshold and standing time based on guidelines for clinical assessment used by experienced anesthesiologists. See Appendix A for more details.

## 5.2 Experimental Setup

We randomly select 70% of all the surgery cases for the model training, setting aside 10% as a validation set for hyperparameter tuning and the other 20% for model testing. We also make sure that all data points from the same surgery case stay in the same subset of data. We follow [Lundberg *et al.*, 2018] and set the prediction horizon as  $W_h = 5$  min, given that it is short enough for a model to capture relevant and predictive information of potential future hypoxemia but long enough for clinicians to take actions. See Appendix C for details.

### Evaluation Metrics

We use area under the receiver operating characteristic curve (ROC-AUC) and area under the precision-recall curve (PR-AUC) to evaluate the prediction results. Note that PR-AUC is more informative in evaluating imbalanced datasets [Davis and Goadrich, 2006]. We report the precision and the number of alarms per hour of surgery (Alarm/hr), given a sensitivity (i.e., recall) cut at 80%, where the ground truth alarm rate is given by  $\text{GT-Alarm/hr}@0.8R = 0.8 \times \text{GT-Alarm/hr}$ . GT-Alarm/hr denotes the number of all true alarms per hour.

### Compared Baselines

We compare hiNet to the following classical models, RNN models, and AE based methods where we use the same AE layer configuration as in hiNet:

- **LR**: Logistic Regression. Since LR cannot directly process time series, we follow [Lundberg *et al.*, 2018] to extract the exponentially weighted moving (EWM) features that capture temporal patterns of all history data to train LR.
- **GBM**: Gradient Boosting Machines, used in the state-of-the-art hypoxemia prediction system *Prescience* [Lundberg *et al.*, 2018]. We follow them to use XGBoost [Chen and Guestrin, 2016], a widely-used and effective implementation of GBM. We use the same features in LR to train GBM.



Figure 3: t-SNE visualization and kernel density estimation (scaled) of learned representation by LSTM-AE and hiNet on persistent hypoxemia prediction. (a) encoder output of LSTM-AE; (b) encoder output of hiNet; (c) output of the shared inference layers of hiNet; and (d) output of last hidden layer of the Predictor in hiNet.

- **LSTM**: Vanilla LSTM, a baseline for RNN based models.
- **Deep LSTM**: Using stacked bi-LSTM for feature gathering and an MLP as the classifier, with layers configured the same way as the Predictor in hiNet.
- **LSTM-AE** [Zhu and Laptev, 2017]: A deep LSTM classifier with the weights pretrained on an LSTM-AE.
- **LSTM-CAE** [Srivastava *et al.*, 2015]: A deep LSTM classifier with the weights pretrained on an LSTM-CAE that jointly reconstructs input and forecasts future input.

We only use intraoperative time series in the above methods and hiNet. To explore the effect of incorporating preoperative features (e.g., age, sex, and weight), we further collect 9 preoperative variables for the same patient cohort we have, and add these static features to the input of GBM as in [Lundberg *et al.*, 2018] (**GBM + PreOp**). For hiNet, we concatenate the preoperative features with the data representation  $\mathbf{p}_{i,t}$  in Eq. (8) as the classifier input (**hiNet + PreOp**).

## 5.3 Result and Discussion

### General Performance

To answer question **Q1**, we report the performance on the two tasks in Table 1, and make the following observations: (i) hiNet significantly outperforms all baselines on both tasks, which shows the effectiveness of joint learning and memory embedding for rare event prediction. (ii) Compared to GBM+PreOp used by the state-of-the-art system *Prescience* [Lundberg *et al.*, 2018], hiNet+PreOp yield **68.4% and 82.63% improved PR-AUC** in predicting general and

Method	Persistent Hypoxemia ( $\geq 10$ min)				General Hypoxemia ( $\geq 1$ min)			
	ROC-AUC	PR-AUC	Precision@0.8R	# Alarm/hr	ROC-AUC	PR-AUC	Precision@0.8R	# Alarm/hr
LR	0.9597 (.000)	0.0341 (.003)	0.0092 (.002)	1.93 (.44)	0.8701 (.001)	0.1326 (.004)	0.0461 (.001)	13.35 (.29)
GBM	0.9690 (.000)	0.0670 (.001)	0.0147 (.001)	1.21 (.08)	0.9078 (.000)	0.1904 (.001)	0.0654 (.001)	9.41 (.14)
LSTM	0.9996 (.000)	0.5164 (.024)	0.3436 (.035)	0.05 (.00)	0.9925 (.000)	0.8785 (.001)	0.9712 (.001)	0.63 (.00)
Deep LSTM	0.9996 (.000)	0.6576 (.012)	0.4478 (.023)	0.04 (.00)	0.9925 (.000)	0.8753 (.002)	0.9580 (.001)	0.64 (.00)
LSTM-AE	0.9995 (.000)	0.7021 (.012)	0.6467 (.014)	0.03 (.00)	0.9927 (.000)	0.8896 (.003)	0.9773 (.001)	0.63 (.00)
LSTM-CAE	0.9996 (.000)	0.7062 (.013)	0.6425 (.027)	0.03 (.00)	0.9927 (.000)	0.8901 (.001)	0.9849 (.001)	0.62 (.00)
hiNet <sup>F</sup>	0.9999 (.000)	0.8687 (.013)	0.7664 (.035)	0.02 (.00)	0.9926 (.000)	0.8895 (.001)	0.9924 (.003)	0.62 (.00)
hiNet <sup>Mem</sup>	0.9999 (.000)	0.8539 (.015)	0.6982 (.024)	0.03 (.00)	0.9924 (.000)	0.8855 (.001)	0.9806 (.004)	0.63 (.00)
hiNet <sup>Share</sup>	0.9999 (.000)	0.8740 (.013)	0.7519 (.037)	0.02 (.00)	0.9925 (.000)	0.8881 (.003)	0.9858 (.008)	0.62 (.00)
hiNet <sup>Mask</sup>	0.9999 (.000)	0.8804 (.017)	0.7706 (.018)	0.02 (.00)	0.9926 (.000)	0.8895 (.002)	0.9934 (.004)	0.62 (.00)
hiNet	1.0000 (.000)	0.9219 (.007)	0.8681 (.020)	0.02 (.00)	0.9927 (.000)	0.8904 (.001)	0.9936 (.003)	0.62 (.00)
GBM + PreOp	0.9735 (.000)	0.1021 (.001)	0.0235 (.002)	0.75 (.06)	0.9143 (.000)	0.2064 (.001)	0.0712 (.001)	8.65 (.12)
hiNet + PreOp	1.0000 (.000)	0.9284 (.009)	0.8785 (.026)	0.02 (.00)	0.9934 (.000)	0.8904 (.002)	0.9919 (.002)	0.62 (.00)

Table 1: Prediction results on the two tasks. The ground truth GT-Alarm/hr@0.8R is **0.02** (persistent) and **0.62** (general).

persistent hypoxemia. By incorporating preoperative features, both GBM and hiNet improve in performance. RNN based models outperform LR and GBM by a large margin, as generally RNN is better at learning temporal patterns in time series. (iii) Pretraining (e.g., LSTM-AE) gives a large performance gain over the models trained from scratch (e.g., LSTM), which shows that the sequence AE network does help learn a good representation that improves the classification. hiNet further improves LSTM-CAE by using memory embedding and joint training. (iv) Throughout, predicting persistent hypoxemia is much harder than predicting general hypoxemia, which requires a model to capture extremely rare patterns or foresee farther future. Most baselines perform worse on this harder task, while hiNet handles both of the tasks well. In hiNet, the learned future-indicative representation potentially improves the robustness against class imbalance. (v) In every 100 hours of surgery, hiNet produces 2 alarms and 62 alarms for persistent and general hypoxemia, which are very close to the ground truth. With high precision, hiNet produces exceptionally low rate of false alarms, which effectively improves the efficacy of alerts.

#### Ablation Study

To answer question Q2, we analyze the contribution of each component in hiNet by removing it. We evaluate the following hiNet variants, as shown in Table 1: (i) **hiNet<sup>Mem</sup>**: We replace the memory layers with two stacked independent linear layers. The result shows memory embedding helps learn better latent representation that facilitates the classification. (ii) **hiNet<sup>F</sup>**: hiNet with Forecaster  $f_F$  removed. We observe that the future-indicative patterns extracted through Forecaster contributes to better classification performance. (iii) **hiNet<sup>Share</sup>**: The shared inference layers that connects Forecaster and Predictor in hiNet are replaced with two separate MLPs. We observe that Predictor benefits better from Forecaster in learning future-indicative patterns via the exclusively shared bottleneck. (iv) **hiNet<sup>Mask</sup>**: Directly excluding unlabeled training examples, the same way we train baselines such as GBM and LSTM. We observe that by using the masked loss for Predictor, the unlabeled data still contribute to the representation learning through Reconstructor and Forecaster, although not used by Predictor.

#### Representation Learning

To answer question Q3, we extracted the latent representation learned by LSTM-AE and various layers of hiNet for persistent hypoxemia prediction, and visualize these vectors in a 2D space using t-SNE [Van Der Maaten, 2014]. Considering the extreme class imbalance, we randomly select 50 surgeries where persistent hypoxemia occurred and 50 hypoxemia-free cases from the test set for visualization purpose. As shown in Figure 3, the representation of the same class in the code space tends to group together in hiNet, which enlarges the partitioning margin and makes them easier to classify. Clearer grouping patterns can be observed at layers closer to the Predictor output with stronger supervisory signal. In contrast, the representation learned by an LSTM-AE is structured but shows much less salient grouping patterns. We observe that, hiNet is able to learn powerful task-specific representation via joint training and memory embedding, where supervisory signal is propagated to fine-tune latent representation towards task-specific effectiveness.

#### 6 Conclusion and Clinical Significance

We developed a novel end-to-end learning approach based on a joint sequence autoencoder, for near-term prediction of hypoxemia, especially persistent hypoxemia, a rare but critical adverse surgical condition of high clinical significance. In a large dataset of surgeries from a major academic medical center, our proposed model achieves a precision of 99.36% and 86.81% in predicting general and persistent hypoxemia, respectively, at 80% sensitivity, which significantly outperforms strong baselines including the model used by the state-of-the-art hypoxemia prediction system. With exceptional precision, our method produces very low rate of false alarms, which helps improve the efficacy of alerts. This work has the potential to impact clinical practice by predicting clinically significant intraoperative hypoxemia and facilitating timely interventions. By tackling the challenging problem of predicting rare, but critical persistent hypoxemia, our model could help preventing adverse patient outcomes. Although developed to target hypoxemia, our model and approach could potentially generalize to similar problems such as predicting intraoperative hypotension.

## References

- [Ballinger *et al.*, 2018] Brandon Ballinger, Johnson Hsieh, Avesh Singh, Nimit Sohoni, Jack Wang, Geoffrey Tison, Gregory Marcus, Jose Sanchez, Carol Maguire, Jeffrey Olgin, et al. Deepheart: semi-supervised sequence learning for cardiovascular risk prediction. In *AAAI*, volume 32, 2018.
- [Baytas *et al.*, 2017] Inci M Baytas, Cao Xiao, Xi Zhang, Fei Wang, Anil K Jain, and Jiayu Zhou. Patient subtyping via time-aware lstm networks. In *KDD*, pages 65–74, 2017.
- [Chen and Guestrin, 2016] Tianqi Chen and Carlos Guestrin. Xgboost: A scalable tree boosting system. In *KDD*, pages 785–794, 2016.
- [Dai and Le, 2015] Andrew M Dai and Quoc V Le. Semi-supervised sequence learning. *NeurIPS*, 28:3079–3087, 2015.
- [Davis and Goadrich, 2006] Jesse Davis and Mark Goadrich. The relationship between precision-recall and roc curves. In *ICML*, pages 233–240, 2006.
- [Dunham *et al.*, 2014] C Michael Dunham, Barbara M Hileman, Amy E Hutchinson, Elisha A Chance, and Gregory S Huang. Perioperative hypoxemia is common with horizontal positioning during general anesthesia and is associated with major adverse outcomes: a retrospective study of consecutive patients. *BMC anesthesiology*, 14(1):1–10, 2014.
- [Ehrenfeld *et al.*, 2010] Jesse M Ehrenfeld, Luke M Funk, Johan Van Schalkwyk, Alan F Merry, Warren S Sandberg, and Atul Gawande. The incidence of hypoxemia during surgery: evidence from two institutions. *Canadian Journal of Anesthesia*, 57(10):888–897, 2010.
- [ElMoaqet *et al.*, 2016] H. ElMoaqet, D. M. Tilbury, and S. K. Ramachandran. Multi-step ahead predictions for critical levels in physiological time series. *IEEE Transactions on Cybernetics*, 46(7):1704–1714, 2016.
- [Erion *et al.*, 2017] Gabriel Erion, Hugh Chen, Scott M Lundberg, and Su-In Lee. Anesthesiologist-level forecasting of hypoxemia with only spo2 data using deep learning. In *NeurIPS Workshop ML4H*, 2017.
- [Gong *et al.*, 2019] Dong Gong, Lingqiao Liu, Vuong Le, Budhaditya Saha, Moussa Reda Mansour, Svetha Venkatesh, and Anton van den Hengel. Memorizing normality to detect anomaly: Memory-augmented deep auto-encoder for unsupervised anomaly detection. In *ICCV*, pages 1705–1714, 2019.
- [Hendrycks *et al.*, 2019] Dan Hendrycks, Kimin Lee, and Mantas Mazeika. Using pre-training can improve model robustness and uncertainty. *ICML*, 2019.
- [Laffin *et al.*, 2020] Anton E Laffin, Samir M Kendale, and Tessa Kate Huncke. Severity and duration of hypoxemia during outpatient endoscopy in obese patients: a retrospective cohort study. *Canadian Journal of Anaesthesia*, 2020.
- [Laptev *et al.*, 2017] Nikolay Laptev, Jason Yosinski, Li Er-ran Li, and Slawek Smyl. Time-series extreme event forecasting with neural networks at uber. In *ICML*, volume 34, pages 1–5, 2017.
- [Lundberg *et al.*, 2018] Scott M. Lundberg, Bala Nair, Monica S. Vavilala, Mayumi Horibe, Michael J. Eisses, Trevor Adams, David E Liston, Daniel King-Wai Low, Shu-Fang Newman, Jerry Kim, et al. Explainable machine-learning predictions for the prevention of hypoxaemia during surgery. *Nature Biomedical Engineering*, 2(10):749–760, 2018.
- [Mehta and Mehta, 2016] Chitra Mehta and Yatin Mehta. Management of refractory hypoxemia. *Annals of cardiac anaesthesia*, 19(1):89, 2016.
- [Nguyen *et al.*, 2018] Hung Nguyen, Sooyong Jang, Radoslav Ivanov, Christopher P Bonafide, James Weimer, and Insup Lee. Reducing pulse oximetry false alarms without missing life-threatening events. *Smart Health*, 9:287–296, 2018.
- [Santoro *et al.*, 2016] Adam Santoro, Sergey Bartunov, Matthew Botvinick, Daan Wierstra, and Timothy Lillicrap. Meta-learning with memory-augmented neural networks. In *ICML*, pages 1842–1850, 2016.
- [Srivastava *et al.*, 2015] Nitish Srivastava, Elman Mansimov, and Ruslan Salakhudinov. Unsupervised learning of video representations using lstms. In *ICML*, pages 843–852, 2015.
- [Sukhbaatar *et al.*, 2015] Sainbayar Sukhbaatar, Jason Weston, Rob Fergus, et al. End-to-end memory networks. In *NeurIPS*, pages 2440–2448, 2015.
- [Suresh *et al.*, 2017] Harini Suresh, Peter Szolovits, and Marzyeh Ghassemi. The use of autoencoders for discovering patient phenotypes. *NeurIPS Workshop ML4H*, 2017.
- [Tang *et al.*, 2020] Xianfeng Tang, Huaxiu Yao, Yiwei Sun, Charu C Aggarwal, Prasenjit Mitra, and Suhang Wang. Joint modeling of local and global temporal dynamics for multivariate time series forecasting with missing values. In *AAAI*, pages 5956–5963, 2020.
- [Van Der Maaten, 2014] Laurens Van Der Maaten. Accelerating t-sne using tree-based algorithms. *JMLR*, 15(1):3221–3245, 2014.
- [West *et al.*, 2016] Colin P West, Liselotte N Dyrbye, Patricia J Erwin, and Tait D Shanafelt. Interventions to prevent and reduce physician burnout: a systematic review and meta-analysis. *The Lancet*, 388(10057):2272–2281, 2016.
- [Zhou *et al.*, 2014] Yingbo Zhou, Devansh Arpit, Ifeoma Nwogu, and Venu Govindaraju. Is joint training better for deep auto-encoders? *arXiv preprint arXiv:1405.1380*, 2014.
- [Zhu and Laptev, 2017] L. Zhu and N. Laptev. Deep and confident prediction for time series at uber. In *ICDM Workshop*, pages 103–110, 2017.

# Appendices

## A Hypoxemia Definition and Labeling

We use a stringent clinical definition of hypoxemia to assess a patient encounter during surgery. We define the two types of hypoxemia and assign labels for the two prediction problems following the criteria as shown in Figure 5. The regions in red where  $\text{SpO}_2 > 90\%$  represent a normal state of a patient. The dark purple region with  $\text{SpO}_2 \leq 90\%$  that consecutively lasts for at least 10 min stands for a persistent hypoxemia (also belonging to general hypoxemia) event. The light purple region with at least one continuous  $\text{SpO}_2 \leq 90\%$  stands for general hypoxemia.

In our dataset, the prevalence of general hypoxemia was 1.5% of all surgery time, with 24.0% of the patient encounters experienced at least once during surgery. However, the prevalence of persistent hypoxemia was 0.6% of the total surgery time, with merely 0.9% of the patient encounters experienced persistent hypoxemia at least once.

Figure 5 shows the hypoxemia labeling for classifier training. For each prediction problems, given a 5 min horizon, we assign positive labels to the time steps within this 5 min predictive window right before the start of a hypoxemic event (persistent or general hypoxemia, respectively). Other time steps prior to this predictive window are assigned with negative labels. We leave the samples during the time window when the patient is already in a hypoxemic event unlabeled, as it has little clinical benefit to predict hypoxemia when hypoxemia already occurs.

## B Assumptions

It is important to note that, when producing labels for clinical outcomes such as hypoxemia, anaesthesiologist interventions can indirectly affect the prediction outcome [Lundberg *et al.*, 2018]. As these interventions may affect certain vital parameters including  $\text{SpO}_2$ , models that use these parameters can learn when a doctor is likely to intervene and hence lower the risk of a potential high-risk patient. The ideal solution to this issue is to remove all samples where clinicians have intervened for model training. But this is difficult in practice, since fully identifying when clinicians are taking hypoxemia-preventing interventions is not possible. Hence, our model as all other previous learning based approaches [Lundberg *et al.*, 2018; Erion *et al.*, 2017] to this problem, must be based on the natural assumption that the model predicts hypoxaemia when clinicians are following standard procedures, including (possibly) taking interventions to prevent potential hypoxemia anticipated based on clinician’s professional knowledge.

## C Implementation Details

For persistent hypoxemia ( $\geq 10$  min) prediction, we set the observation window  $W_o = 20$  min and the horizon of Forecaster  $L = W_h + 10 = 15$ . For general hypoxemia ( $\geq 1$  min) prediction, we set  $W_o = 10$  and  $L = W_h + 1 = 6$ . The notion is that, given a 5 min prediction horizon, we need to see 15 min ahead to the future to speculate persistent hypoxemia and only 6 min for single  $\text{SpO}_2$  drops.

We use bidirectional LSTM (bi-LSTM) for all LSTM layers in hiNet for its powerful representation capacity. Each MLP in hiNet has only one hidden layer with rectified linear unit (ReLU) as the activation function. The number of neurons for each hidden layer in both LSTM and MLP, and the number of basis  $M$  in the memory are all set as 128. We select the regularizer coefficient  $\beta$  from  $\{10^{-4}, 10^{-3}, 10^{-2}, 10^{-1}, 10^0, 10^1\}$ .

We use Adam as the optimizer and train the model with mini batches. For each batch, we feed 128 independent surgeries containing on average about 11,400 extracted examples into the model. We use the same settings for all RNN based baselines and all variants of hiNet. All of them are trained for 80 epochs with early stopping and drop-out applied to prevent overfitting. The model with the lowest epoch-end classification loss at each run is saved and evaluated with test data.

## D Hyperparameter Analysis

We investigate the sensitivity of hyperparameter  $\beta$ , which balances the Predictor loss and the regularization of Reconstructor and Forecaster. Generally, as  $\beta$  increases from a very small value, the joint model would converge with smaller reconstruction and forecasting errors, which help the classifier learn better representation. However, when  $\beta$  is too large, too much emphasis is put on the regularization components while the Predictor may not be thoroughly trained. We alter the value of  $\beta$  among  $\{10^{-4}, 10^{-3}, 10^{-2}, 10^{-1}, 10^0, 10^1\}$  and report the PR-AUC, as ROC-AUC would stay a high value and change little given the extreme class imbalance. As shown in Figure 4, the performance of hiNet in predicting persistent hypoxemia first increase and then decline as  $\beta$  increases. That justifies the regularization effect of Reconstructor and Forecaster. In predicting general hypoxemia, hiNet is relatively less sensitive to  $\beta$ , given a relatively simpler problem that has higher baseline performance.

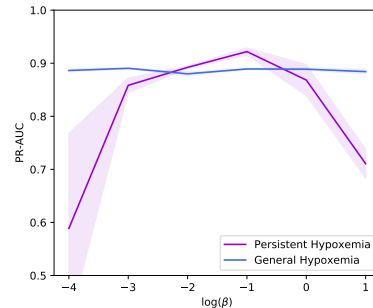


Figure 4: Prediction performance (PR-AUC) with different  $\beta$ .

## E Alternative Strategy: Hypoxemia Prediction via $\text{SpO}_2$ Forecasting

Since the risk of potential hypoxemia strongly relates to future  $\text{SpO}_2$  levels, a natural strategy of predicting hypoxemia would be forecasting future  $\text{SpO}_2$  sequence. In addition to direct classification, we further investigate this alternative strat-

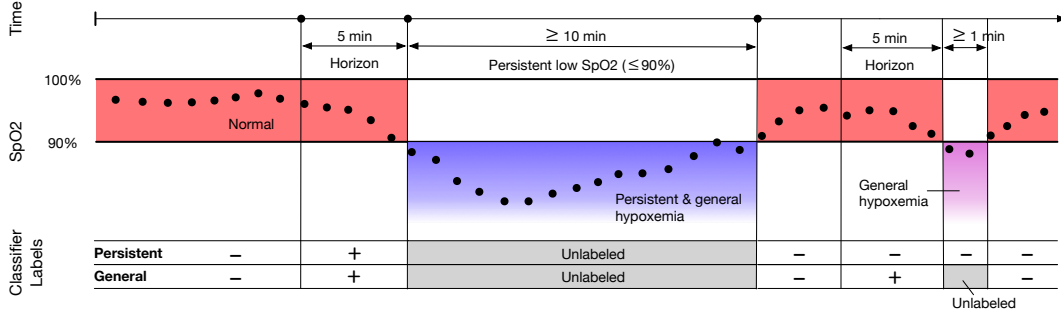


Figure 5: Definition of hypoxemia of two severeness levels and their label assignment. For unlabeled data, data mask  $m_{i,t} = 0$ .

egy where we first build a regressive model to forecast the future  $SpO_2$  using all vitals and then detect persistent hypoxemia or general hypoxemia based on the estimated future  $SpO_2$  levels. We compare the direct classification results of hiNet to the following methods based on this strategy:

- **VAR**: Vector autoregression, a statistical model used to capture temporal patterns in multivariate time series.
- **LSTM-AE** [Zhu and Laptev, 2017]: Use LSTM-AE directly for  $SpO_2$  sequence forecasting with the encoder pretrained via reconstructing the input time series.
- **LSTM-CAE** [Srivastava *et al.*, 2015]: Use LSTM-CAE to jointly reconstruct all channels of input vitals and forecast future  $SpO_2$  sequences.
- **LGnet** [Tang *et al.*, 2020]: State-of-the-art memory based multivariate time series forecasting approach with adversarial training. LGnet is capable of handling missing values directly, so we don't apply imputation for it.
- **hiNet<sup>P</sup>**: Modified hiNet with Forecaster  $f_F$  purely forecasting  $SpO_2$  sequence and Predictor  $f_P$  removed.

The horizon  $L$  of LSTM-AE, LSTM-CAE and hiNet<sup>P</sup> is set as 6 min and 11 min for general and persistent hypoxemia. VAR and LGnet recursively forecast the next-step values and use the estimated values as input for later estimations. Besides sensitivity and precision, root means square error (RMSE) is used to evaluate the estimation of future  $SpO_2$  (one value for general hypoxemia and 10-min sequence for persistent hypoxemia). Tables 2 and 3 shows the results of predicting persistent hypoxemia and general hypoxemia via future  $SpO_2$  forecasting, in contrast to the direct classification result of hiNet. We can see that even though time series forecasting methods such as LGnet achieve low error in future  $SpO_2$  estimation, the performance on sensitivity and precision of hypoxemia prediction still turns out poor. The events of persistent hypoxemia or general hypoxemia are so rare that the regression models fail to capture the pattern of consecutive low  $SpO_2$ . Here a small RMSE of  $SpO_2$  estimation does not reflect accurate forecast of low  $SpO_2$  ( $\leq 90\%$ ).

## F Features

Table 4 shows the 18 intraoperative physiological time series variables used by all methods including the standard hiNet,

and the 9 preoperative static variables used by the extended methods GBM+PreOp and hiNet+PreOp.

Method	SpO <sub>2</sub> RMSE	Sensitivity	Precision
VAR	0.0283	0.2291	0.0005
LSTM-AE	0.0279	0.2692	0.0007
LSTM-CAE	0.0235	0.5260	0.0011
LGnet	<b>0.0205</b>	<b>0.5310</b>	<b>0.0023</b>
hiNet <sup>P</sup>	<u>0.0233</u>	0.4199	0.0009
hiNet	N.A.	0.8	0.8573

Table 2: Results of **persistent hypoxemia** prediction via  $SpO_2$  forecasting on the two tasks (for RMSE the lower the better).

Method	SpO <sub>2</sub> RMSE	Sensitivity	Precision
VAR	0.0221	0.3109	0.0224
LSTM-AE	0.0218	0.3315	0.0238
LSTM-CAE	<u>0.0181</u>	0.3716	0.0294
LGnet	<b>0.0138</b>	<b>0.4210</b>	<b>0.0468</b>
hiNet <sup>P</sup>	0.0182	<u>0.3734</u>	<u>0.0296</u>
hiNet	N.A.	0.8	0.9949

Table 3: Results of **general hypoxemia** prediction via  $SpO_2$  forecasting on the two tasks (for RMSE the lower the better).

Intraoperative Time Series	Preoperative Variable
Invasive blood pressure, diastolic	Age
Invasive blood pressure, mean	Height
Invasive blood pressure, systolic	Weight
Noninvasive blood pressure, diastolic	Sex
Noninvasive blood pressure, mean	ASA physical status
Noninvasive blood pressure, systolic	ASA emergency status
Heart rate	Surgery type
SpO <sub>2</sub>	Second hand smoke
Respiratory rate	Operating room
Positive end expiration pressure (PEEP)	
Peak respiratory pressure	
Tidal volume	
Pulse	
End tidal CO <sub>2</sub> (ETCO <sub>2</sub> )	
O <sub>2</sub> flow	
N <sub>2</sub> O flow	
Air flow	
Temperature	

Table 4: List of intraoperative and preoperative features.